Importance of classical diffusion in NMR studies of water in biological cells

K. R. Brownstein and C. E. Tarr
Department of Physics and Astronomy, University of Maine, Orono, Maine 04469
(Received 29 September 1978)

Nuclear-magnetic-resonance measurements of the proton-spin relaxation for water in biological cells are known to exhibit a multiexponential decay. A theory, based on the diffusion equation using the bulk diffusivity of water, is developed to explain this phenomenon. It is shown that multiexponential decay arises simply as a consequence of an eigenvalue problem associated with the size and shape of the cell and that this multiexponential decay can only be observed for samples whose size is of the order of a biological cell. As an example, the theory is applied to a previously published data for rat gastronemius cells. Excellent agreement is obtained, and furthermore, the size of the cell is calculated by fitting the theory to the experiment.

I. INTRODUCTION

Proton spin-spin and spin-lattice relaxation in water in biological cells appears to be quite different from that observed for bulk water. In particular, the relaxation times are considerably shorter than those in bulk water and the relaxation cannot be described by a single-exponential process.[1] A number of theories have been proposed to explain these phenomena which make use of detailed properties of the cell; some theories necessitate altered properties of the intracellular water, such as "bound" water, specific interactions with membrances, and free macromolecules.[2-8]

In this paper, we develop a simple explanation to account for the proton magnetic relaxation in such systems. In this model[9] only the properties of bulk water are used. Further, it is shown that the multiexponential nature of the relaxation is a consequence of the geometry of the cells. In particular, it is possible to infer reasonable estimates of both the shape and size of the cells from NMR data alone.

In our model we consider an initial state in which the nuclear magnetization is uniform throughout the water in the cell. The evolution of the system is then governed by two properties: (a) paramagnetic materials acting as relaxation centers, and (b) classical diffusion of the water molecules with the diffusion constant characteristic of bulk water.

II. THEORY

A. Normal mode analysis

Consider a sample (e.g., a biological cell) of volume V of water having a magnetic moment per unit volume (along some specified direction) $\rho(\vec{r}, t)$. Experimentally, one measures an electronic signal proportional to the total nuclear magnetization of the sample

$$\mathfrak{M}(t) = \int_V \rho(\vec{r}, t)\, d\tau \,. \tag{1}$$

This magnetization can decay due to a volumelike sink characterized by a sink strength density $\gamma(\vec{r}) \geq 0$ in an "active volume" v and a surfacelike sink characterized by a sink strength density $\mu(\vec{r}) \geq 0$ on an "active surface" s. In what follows we shall take $\mathfrak{M}(t)$ to mean the reduced magnetization. For example, in the case of 180°-90° T_1 measurement

$$\mathfrak{M}(t) = [S(\infty) - S(t)]/[2S(\infty)] ,$$

where $S(t)$ is the observed signal at time t and $S(\infty)$ is the equilibrium value of S. The physical nature of these sinks will not be dealt with here, but one can hypothesize magnetic impurities such as macromolecules, bound water, etc.

The governing equations for the above situation are

$$\vec{\nabla} \cdot (\vec{D} \cdot \vec{\nabla}\rho) - \gamma\rho = \frac{\partial \rho}{\partial t} \,, \tag{2}$$

$$(\hat{n} \cdot \vec{D} \cdot \vec{\nabla}\rho + \mu\rho)\big|_S = 0 \,, \tag{3}$$

$$\rho(\vec{r}, 0) = \mathfrak{M}(0)/V \,. \tag{4}$$

Equation (2) is the diffusion equation allowing for the volumelike sink, Eq. (3) is the boundary condition on the bounding surface S taking into account the surfacelike sink, and Eq. (4) is the presumed initial condition corresponding to an initial uniform magnetization of the sample. The symbols employed here and in what follows are $\rho(\vec{r}, t)$: magnetic moment per unit volume (* cm^{-3}); V:

sample volume (cm^3); v: active volume (cm^3): $d\tau$: volume element (cm^3); S: sample surface (cm^2); s: active surface (cm^2); df: surface element (cm^2); $\gamma(\vec{r})$: volume sink strength density (s^{-1}); $\mu(\vec{r})$: surface sink strength density ($cm\,s^{-1}$); $\Gamma = (1/v)\int \gamma(\vec{r})\,d\tau$: average value of γ over the active volume v (s^{-1}); $M = (1/s)\int \mu(\vec{r})\,df$: average value of μ over the active surface s ($cm\,s^{-1}$); $\mathfrak{M}(t) = \int \rho(\vec{r}, t)\,d\tau$: total nuclear magnetization of sample (*); $\vec{\mathrm{D}}(\vec{r})$: diffusivity tensor ($cm^2\,s^{-1}$); $\hat{n}$: unit outward normal at the bounding surface. Here typical cgs units have been indicated in the parentheses; the * denotes any convenient unit, e.g., erg/G, for magnetic moment.

The solution to the above diffusion problem can be expressed as a sum of "normal modes,"

$$\rho(\vec{r}, t) = \sum_{n=0}^{\infty} A_n F_n(\vec{r}) e^{-t/T_n}. \tag{5}$$

Here the A_n are constants and the orthogonal spatial eigenfunctions $F_n(\vec{r})$ satisfy the positive definite eigenvalue problem

$$-\vec{\nabla}\cdot(\vec{\mathrm{D}}\cdot\vec{\nabla}F_n) + \gamma F_n = (1/T_n)F_n \tag{6}$$

for the boundary condition

$$(\hat{n}\cdot\vec{\mathrm{D}}\cdot\vec{\nabla}F_n + \mu F_n)\,|_S = 0. \tag{7}$$

The eigenvalues, $1/T_n$, appearing in Eq. (6) can be ordered such that

$$T_0 > T_1 \geq T_2 \geq T_3 \geq \cdots > 0. \tag{8}$$

Note that the index n refers to the mode number; T_n is actually $(T_1)_n$ for the case of spin-lattice relaxation or $(T_2)_n$ for the case of spin-spin relaxation. The lowest (in terms of $1/T_n$) mode is assigned the index $n=0$; this mode is always nondegenerate.

The constants A_n in (5) can be evaluated using the initial condition (4) and the orthogonality of the F_n,

$$A_n = \frac{\mathfrak{M}(0)}{V}\,\frac{\int F_n(\vec{r})\,d\tau}{\int F_n^2(\vec{r})\,d\tau}. \tag{9}$$

The observed quantity (1) becomes a sum of decreasing exponential functions of time:

$$\mathfrak{M}(t) = \mathfrak{M}(0)\sum_{n=0}^{\infty} I_n e^{-t/T_n}, \tag{10}$$

where the nth relative intensity, I_n, is given by

$$I_n = \frac{1}{V}\,\frac{[\int F_n(\vec{r})\,d\tau]^2}{\int F_n^2(\vec{r})\,d\tau} \geq 0. \tag{11}$$

Note that these relative intensities are normalized such that

$$\sum_{n=0}^{\infty} I_n = 1. \tag{12}$$

B. Examples

In this section three simple solvable geometries are considered. For each of them there is a surfacelike sink strength density $\mu = M = \text{const}$ over an active surface s. The volumelike sinks are assumed to be absent, i.e., $\gamma = 0$ everywhere. The diffusivity tensor is taken to be homogeneous and isotropic, i.e., $\vec{\mathrm{D}} = D\vec{1}$, where D is constant.

1. Planar geometry

The region is bounded by the planes $z=0$ and $z=a$. The active surface is the $z=a$ face. Only those modes having no x or y dependence contribute. The results for the eigenfunctions F_n, the decay times T_n, and the relative intensities I_n are

$$F_n = \cos(\xi_n z/a), \tag{13a}$$

$$T_n = a^2/D\xi_n^2, \tag{13b}$$

$$I_n = 4\sin^2\xi_n/\xi_n[2\xi_n + \sin(2\xi_n)], \tag{13c}$$

where the ξ_n ($n=0,1,2,\ldots$) are the positive roots (ordered according to value) of the transcendental equation

$$\xi_n \tan\xi_n = Ma/D. \tag{13d}$$

2. Cylindrical geometry

The region is the interior of the cylinder $r=a$. The surface $r=a$ is the active surface. Only those modes having no θ or z dependence contribute. The results (in terms of cylindrical Bessel functions) are

$$F_n = J_0(\eta_n r/a), \tag{14a}$$

$$T_n = a^2/D\eta_n^2, \tag{14b}$$

$$I_n = 4J_1^2(\eta_n)/\eta_n^2[J_0^2(\eta_n) + J_1^2(\eta_n)], \tag{14c}$$

where the η_n are the positive roots of

$$\eta_n J_1(\eta_n)/J_0(\eta_n) = Ma/D. \tag{14d}$$

3. Spherical geometry

The region is the interior of the sphere $r=a$. The surface $r=a$ is the active surface. Only those modes having no θ or ϕ dependence contribute. The results are

$$F_n = \sin(\zeta_n r/a)/(\zeta_n r/a), \tag{15a}$$

$$T_n = a^2/D\zeta_n^2, \tag{15b}$$

$$I_n = \frac{12(\sin\zeta_n - \zeta_n\cos\zeta_n)^2}{\zeta_n^3[2\zeta_n - \sin(2\zeta_n)]}, \tag{15c}$$

where the ζ_n are the positive roots of

$$1 - \zeta_n\cot\zeta_n = Ma/D. \tag{15d}$$

Figures 1 and 2 show some of the results obtained for these examples. In Fig. 1 we show the ratio T_n/T_0 of the nth mode decay time to that of the lowest mode for $n=1,2$. In Fig. 2 we show the nth relative intensity I_n for $n=0,1,2$. From these graphs and Eqs. (13)–(15) certain conclusions can be drawn concerning the general behavior of a system of this type (i.e., one with simple geometry and no volumelike sinks).

The decay times T_n and the relative intensities I_n are determined by a dimensionless eigenvalue ξ_n (or η_n or ζ_n). This eigenvalue spectrum is in turn determined by a dimensionless sink strength parameter Ma/D. There are three qualitatively different regions of behavior according to the value of this parameter.

(a) $Ma/D \ll 1$. This can be called the "fast-diffusion" region and corresponds to the fast-exchange limit of discrete multiphase analysis.[10] Here the lowest mode completely dominates, $I_0 \to 1$. The corresponding decay time for the lowest mode is given by $T_0 = V/ms$ where V is the sample volume and s is the active surface area. This can be seen by taking the appropriate limits in Eqs. (13)–(15) or from more general considerations.[11] The decay times of the higher modes are orders of magnitude smaller than T_0.

(b) $1 \ll Ma/D \ll 10$. This can be called the "intermediate-diffusion" region. The lowest mode still dominates but the higher modes now contribute a few percent to the total relative intensity. The decay times of the first two higher modes are now about one or two orders of magnitude smaller than that of the lowest mode.

(c) $10 \ll Ma/D$. This can be called the "slow-diffusion" region. The majority of the relative intensity is still in the lowest mode (81%, 69%, and 61%, respectively, for the planar, cylindrical, and spherical cases considered); the higher modes contributing a total of a few tens of percent. The decay times of the first two higher modes are only about one order of magnitude smaller than that of the lowest mode.

The functional dependence of the decay times T_n upon the quantities M, a, D, and n is quite similar for all three geometries considered. For the planar case this dependence is shown in Table I. Note that the higher mode decay times T_n ($n \geq 1$) are almost independent of the sink strength density M.

III. GENERAL PROPERTIES OF $\mathfrak{M}(t)$

The observed quantity $\mathfrak{M}(t)$ is a sum of decreasing exponential functions of time with positive relative intensities I_n,

$$\mathfrak{M}(t) = \mathfrak{M}(0) \sum_{n=0}^{\infty} I_n e^{-t/T_n}. \tag{16}$$

One may expect a plot of $\ln[\mathfrak{M}(t)/\mathfrak{M}(0)]$ vs t (here-

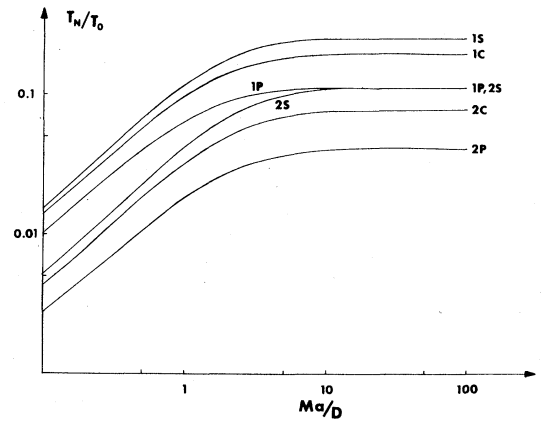

FIG. 1. Ratio of the nth mode decay time to the lowest-mode decay time (T_n/T_0) as a function of the dimensionless sink strength parameter Ma/D. Three geometries (planar, cylindrical, and spherical) are considered; e.g., the notation $2S$ means $n=2$ with spherical geometry.

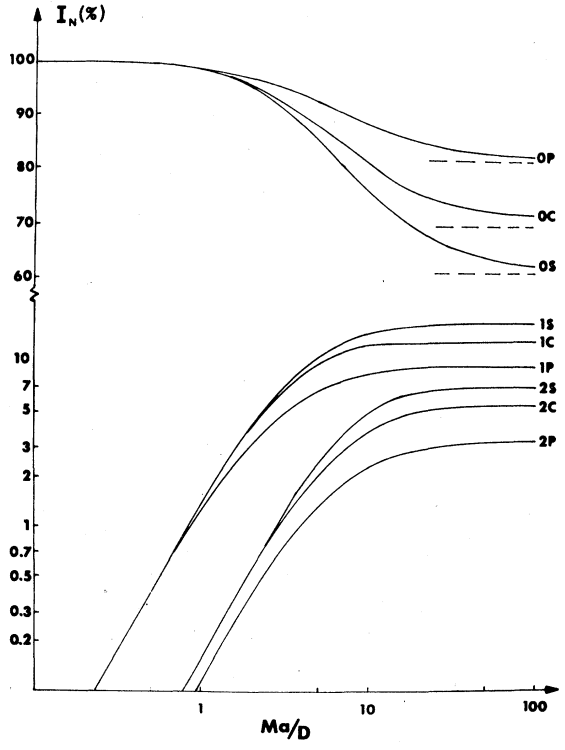

FIG. 2. Relative intensity of the nth mode (I_n) as a function of the dimensionless sink strength parameter Ma/D. The notation is as in Fig. 1. The horizontal dashed lines indicate the asymptotic values of I_0 in the slow diffusion limit ($Ma/D \to \infty$). Note the change of scale for the I_0 curves.

after called the decay curve) to resemble that shown in Fig. 3. This is a multiexponential curve with the majority of the relative intensity being in the lowest mode. In this part we investigate the circumstances under which this multiexponential decay can be discerned from that of a single-exponential decay and how certain integral properties of the sinks affect the shape of the decay curve for small values of t.

In Sec. III A we establish approximate bounds on the possible size of the sample assuming surfacelike sinks only. In Sec. III B, again assuming surfacelike sinks, an equation is derived relating the initial slope of the decay curve to the sink strength parameter Ma/D. Finally in Sec. III C, it is shown how the initial curvature of the decay curve is related to the volume of any volumelike sink.

A. Bounds on the sample size

In order to see the effects of the higher modes it is necessary that one operate in the slow (or at worst, intermediate) diffusion region. Otherwise, the higher mode relative intensities are much too small (see Fig. 2). The observationally possible decay times are limited by the inequalities

$$T_{\min} \ll T_n \ll T_{\max}, \tag{17}$$

for all modes n of interest. Here $T_{\min}$ and $T_{\max}$ are the experimental limits for observation of decay times. Using (a) $n=0,1,2$ (i.e., the three lowest modes), (b) $T_{\min}=1$ μs (a reasonable limit for pulsed NMR techniques), (c) $T_{\max}=2$ s (the approximate value of the intrinsic decay time of bulk water), (d) $T_n=a^2/D(n+\frac{1}{2})^2\pi^2$ (i.e., slow diffusion, planar geometry), (e) $D=2.5\times10^{-5}$ cm^2 s^{-1} (diffusivity of water), and (f) "$\ll$" signs in (17) to mean a factor of 10, one can solve for the sample size limits. The result is

$$1 \leq a \leq 30 \ \mu\text{m}. \tag{18}$$

We see that it is *precisely* in the biological-cell size range that one must look to see the multiexponential decay. Although derived for the case of planar geometry, it is to be expected that the bounds given in (18) apply to all reasonable geometries involving surfacelike sinks only. [Note that since a square root was taken, an error in $T_{\min}$, $T_{\max}$, or even D of a factor of ~10 would result in the limits (18) changing by only a factor of ~3.]

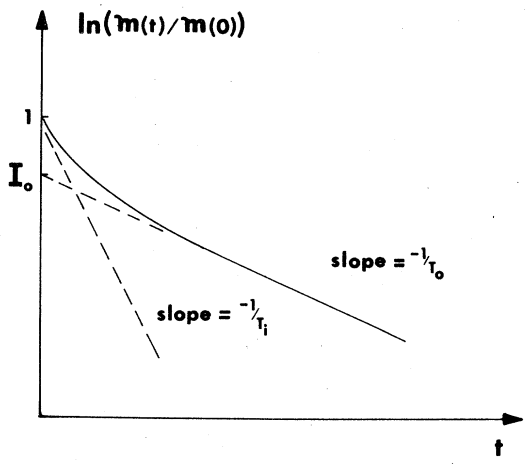

FIG. 3. The expected shape of the decay curve for the slow (or intermediate) diffusion case. T_i is the initial decay time and T_0 is the ultimate (large t) decay time.

B. Initial slope and Ma/D

Even in the very-slow-diffusion limit ($Ma/D \gg 10$) the initial slope of the decay curve remains sensitive to the value of M. To see this, integrate the differential equation (2) over the total volume V for the case of surfacelike sinks only,

$$\int \vec{\nabla} \cdot (\vec{D} \cdot \vec{\nabla}\rho)\, d\tau = \dot{\mathfrak{M}}(t). \tag{19}$$

Transforming the left-hand side into a surface integral, using the boundary condition (3) and the initial condition (4), one obtains

$$\dot{\mathfrak{M}}(0) = \mathfrak{M}(0)\left(\int \mu\, ds\right)/V. \tag{20}$$

Now specializing to the case $\mu = M =$ constant [or defining $M = (\int \mu\, df)/s$ as the average value of μ over the active surface s] one has

$$\dot{\mathfrak{M}}(0)/\mathfrak{M}(0) = Ms/V. \tag{21}$$

But the left-hand side is simply the initial decay rate $1/T_i$, where T_i is the initial effective decay time, thus

$$T_i = V/Ms. \tag{22}$$

[Remark: If there were volumelike sinks present,

TABLE I. Dependence of decay times T_n upon surface sink strength density M, characteristic length dimension of sample a, diffusivity D and mode number n. These expressions are rigorous for planar geometry; similar expressions, differing only by factors of the order unity, hold for cylindrical and spherical geometries.

	Fast diffusion ($Ma/D \ll 1$)	Slow diffusion ($Ma/D \gg 10$)
T_0	a/M	$a^2/[D(0+\frac{1}{2})^2\pi^2]$
$T_n (n \geq 1)$	$a^2/[Dn^2\pi^2]$	$a^2/[D(n+\frac{1}{2})^2\pi^2]$

the above procedure would give

$$T_i = V/(Ms + \Gamma v), \tag{23}$$

where v is the active volume and $\Gamma = (\int \gamma\, d\tau)/v$ is the average value of γ over the active volume v. It is interesting that expression (23) for the *initial* decay time coincides with that for the *single* (constant) decay time in the fast-diffusion limit.[11]]

It is instructive to form the ratio of the large-t decay time T_0 (i.e., that of the lowest mode) to the initial decay time T_i. Using the expressions for T_0 in the three examples considered in Sec. II and Eq. (22) for T_i, one has

$$T_0/T_i = \alpha Ma/D, \tag{24}$$

where $\alpha = 1/\xi_0^2$, $2/\eta_0^2$, $3/\xi_0^2$, respectively, for these three examples. In the slow-diffusion limit, α approaches a number of the order of $\frac{1}{3}$ (0.41, 0.35, 0.31, respectively). Therefore, assuming simple geometry and surfacelike sinks only, one may estimate the dimensionless sink strength parameter Ma/D in the slow-diffusion region using (24) with, say, $\alpha = \frac{1}{3}$. The estimate would be valid only in the slow-diffusion region.

C. Initial curvature and v/V

Assume that there is a volumelike sink $\gamma(\vec{r}) \neq 0$ only in the interior of the region and that there are no surfacelike sinks, i.e., $\mu = 0$. Then the diffusion problem is

$$\vec{\nabla} \cdot \vec{D} \cdot \vec{\nabla}\rho - \gamma\rho = \frac{\partial \rho}{\partial t}, \tag{25a}$$

$$\hat{n} \cdot \vec{D} \cdot \vec{\nabla}\rho\,|_S = 0, \tag{25b}$$

$$\rho(\vec{r}, 0) = \mathfrak{M}(0)/V, \tag{25c}$$

with γ and all its derivatives vanishing on the surface S. By integrating (25a) over the sample volume V and then setting $t = 0$ one obtains an expression for the initial derivative, $\dot{\mathfrak{M}}(0)$, of $\mathfrak{M}(t)$:

$$\dot{\mathfrak{M}}(0)/\mathfrak{M}(0) = -\langle\gamma\rangle, \tag{26}$$

where

$$\langle\gamma\rangle = \frac{1}{V}\int \gamma(\vec{r})\, d\tau \tag{27}$$

is the average value of γ over the entire volume V. [Note that Eqs. (26) and (23) agree since $\langle\gamma\rangle = \Gamma v/V$].

By differentiating (25a) with respect to t and then following the above procedure, one can similarly show that

$$\ddot{\mathfrak{M}}(0)/\mathfrak{M}(0) = +\langle\gamma^2\rangle, \tag{28}$$

where

$$\langle\gamma^2\rangle = \frac{1}{V}\int \gamma^2(\vec{r})\, d\tau. \tag{29}$$

[If any surfacelike sinks were present the value of $\ddot{\mathfrak{M}}(0)$ would have been $+\infty$]. Continuing in this manner, one can obtain expressions for the higher initial derivatives of $\mathfrak{M}(t)$. These turn out not only to involve the average value of a power of γ but also various diffusion terms involving derivatives of γ. For example, the relation for $\dddot{\mathfrak{M}}(0)$ is

$$\dddot{\mathfrak{M}}(0)/\mathfrak{M}(0) = -\langle\gamma^3\rangle - \frac{1}{V}\int \vec{\nabla}\gamma \cdot \vec{D} \cdot \vec{\nabla}\gamma\, d\tau,$$

We shall not pursue the consequences of such higher derivatives since it is difficult enough to determine $\ddot{\mathfrak{M}}(0)$ from experimental data.

If γ is a constant γ_0 in some active volume v and zero elsewhere then

$$\langle\gamma\rangle = \gamma_0 v/V \tag{30a}$$

and

$$\langle\gamma^2\rangle = \gamma_0^2 v/V. \tag{30b}$$

If γ were not constant then Eqs. (30) can be used to *define* an effective value γ_0 of γ and an effective active volume v. Using (26), (28), and (30) one can show that

$$\frac{d}{dt}(T_{\text{eff}})\,\Big|_{t=0} = \frac{V}{v} - 1 \tag{31}$$

where

$$T_{\text{eff}} = -\left(\frac{d}{dt}\{\ln[\mathfrak{M}(t)/\mathfrak{M}(0)]\}\right)^{-1}. \tag{32}$$

is the instantaneous effective decay time (as determined from the slope of the decay curve). This very important result shows that if the initial dimensionless measure of curvature (31) is large, then the effective active volume v occupies but a small fraction of the total sample volume V. If this is the case, then it is supportive evidence for surfacelike sinks since a surfacelike sink can be treated as the limit $v/V \to 0$ of a volumelike sink. (Of course a mathematical surfacelike sink would yield $+\infty$ for the curvature.)

In summary, one can obtain the following information from a decay curve which resembles that in Fig. 3.

(a) Assuming that there are surfacelike sinks only, the experiment must occur in the slow- (or at worst, intermediate-) diffusion region. Otherwise the curve will be essentially a single-exponential decay. Hence $Ma/D \geq 1$.

(b) The value of Ma/D can be estimated from (24) with $\alpha \approx \frac{1}{3}$. A value of $Ma/D \geq 10$ is supportive evidence for slow diffusion; a smaller value of Ma/D would indicate intermediate diffusion.

(c) If one assumes volumelike sinks only, then the ratio v/V of active volume to total volume can be calculated from (31). A small ratio is supportive evidence for surfacelike sinks.

IV. CASE STUDY

In this part we analyze, from the point of view of diffusional modes, a published decay curve of Hazelwood, Chang, Nichols, and Woessner.[1] These data are for spin-spin relaxation of water protons in rat gastronemius muscle. Their results [see their Figures 6(a) and 6(b)] show a fraction (10%) of extracellular water with a characteristic decay time of 155 ms. It is believed that this extracellular water is uncoupled from the remaining intracellular water. Thus the present diffusional-mode theory would predict an $\mathfrak{M}(t)$ given by

$$\mathfrak{M}(t)/\mathfrak{M}(0) = I_{\text{extra}} e^{-t/T_{\text{extra}}} + (1 - I_{\text{extra}}) \times \sum_{n=0}^{\infty} I_n e^{-t/T_n}, \tag{33}$$

where

$$I_{\text{extra}} = 0.10, \tag{34a}$$

$$T_{\text{extra}} = 155 \text{ ms}, \tag{34b}$$

are the relative intensity and decay time of the extracellular water. The next longest decay time in their data is that of their "major fraction" ($\approx 80\%$) of water which we interpret as that of the lowest diffusional mode. This decay time (as measured from their graph) is 45 ms. They also show [in their Fig. 6(c)] that the intercept (due to extracellular plus major fraction) on the $\ln[\mathfrak{M}(t)/\mathfrak{M}(0)]$ axis is -0.11. In our notation this information means that

$$T_0 = 45 \text{ ms}, \tag{35a}$$

$$\ln[I_{\text{extra}} + (1 - I_{\text{extra}}) I_0] = -0.11. \tag{35b}$$

Equation (35b) tells us that the lowest mode relative intensity is $I_0 = 88.4\%$.

Before proceeding further, let us apply the tests (b) and (c) mentioned at the end of Sec. III.

(b) Using $T_i = 5.4$ ms [the value indicated for the initial decay time in their Fig. 6(c)] and $T_0 = 45$ ms, one finds as an estimate for the dimensionless sink strength parameter $Ma/D \approx 25$. This argues strongly for the extreme slow diffusion region for any of the three geometries studied in Sec. II.

(c) It is, of course, very difficult to evaluate the initial curvature [left-hand side of (31)] from the numerical data. Our estimate, as measured from their Fig. 6(c), is that $d(T_{\text{eff}})/dt \approx 50$ at $t = 0$. This would give a volume ratio of $V/v \approx 50$ [the 1 in Eq. (31) is now negligible]. We estimate, more conservatively, that this initial curvature would certainly seem to place the ratio V/v somewhere between 25 and ∞. This evidence supports the hypothesis that the active volume is very small and thus at any rate does not disagree with an assumption of surfacelike sinks only.

On the basis of the above reasoning involving surface sinks, it was decided to try to reproduce their decay curve using each of the three geometries discussed in Sec. II. Each model possesses two parameters: a dimensionless sink strength parameter Ma/D and a time-scale parameter a^2/D. These are used to satisfy Eqs. (35a) and (35b), respectively. It must be emphasized that once Eqs. (35) are satisfied there are *no free parameters*; the decay curve is then uniquely determined. Figure 4 shows the decay curve associated with the cylindrical-geometry case. The planar-geometry case gave a better fit and the spherical-geometry case gave the poorest fit. All three cases exhibit reasonably the correct qualitative behavior; on this basis alone we believe that one is forced to conclude that the effects of these diffusional modes are very important and may indeed be the dominant reason for the observed multiexponential decay in experiments of this type. Quantitatively,

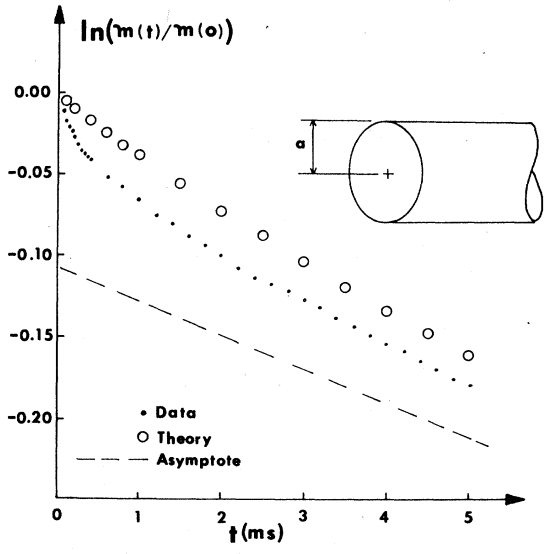

FIG. 4. Decay curve of Hazelwood *et al.* (dots) and its asymptote (dashed line). The open circles are the prediction of the present diffusional theory for the case of a solid cylinder of radius a. The outer surface of the cylinder is active with a surface sink strength parameter given by $Ma/D = 4.44$. This value forces the theory to have the correct asymptote; there are no other free parameters.

however, the initial decay time T_i is too long for all three cases. This is related to the fact that the values of Ma/D [as determined from (35a)] were approximately 8.2, 4.4, and 4.0, respectively, for the planar, cylindrical, and spherical geometries. These values are consistent with the intermediate-diffusion region but are somewhat inconsistent with the extreme slow-diffusion estimate (b) above of $Ma/D \approx 25$.

Noting that the results get better in the geometry sequence (spherical, cylindrical, planar), it was decided to try a geometry which continued this sequence (in the sense that the dominant active surface would now be convex with a larger, perhaps infinite, value of M) and which was a more realistic model of this particular biological cell. The geometry selected is that of an annular cylinder $a \leq r \leq b$ whose inner surface is infinitely active ($\mu = +\infty$ at $r = a$) and whose outer surface is partially active ($\mu = M$ at $r = b$). This model has three parameters: Ma/D, a^2/D and the ratio of radii $R = b/a$. When conditions (35) are satisfied, the model has but *one* remaining free parameter which can be taken to be R. The solution to this diffusion problem is

$$F_n = G_n(\beta_n r/a), \tag{36a}$$

$$T_n = a^2/(D\beta_n^2), \tag{36b}$$

$$I_n = \frac{4}{\beta_n^2(R-1)} \frac{uH_n(u)\,|_{u=\beta_n}^{u=R\beta_n}}{\{u\,[H_n^2(u)+G_n^2(u)]\}\,|_{u=\beta_n}^{u=R\beta_n}}, \tag{36c}$$

where

$$G_n = J_0 - [J_0(\beta_n)/Y_0(\beta_n)]Y_0, \tag{36d}$$

$$H_n = J_1 - [J_0(\beta_n)/Y_0(\beta_n)]Y_1, \tag{36e}$$

with β_n satisfying the transcendental equation

$$-\beta_n H_n(R\beta_n)/G_n(R\beta_n) = Ma/D. \tag{36f}$$

Here J and Y are cylindrical Bessel functions of the first and second kind, respectively.

TABLE II. Properties of the annular cylinder model. The ratio of the radii is $R = b/a = 3$. The inner sink strength density is infinity, the outer sink strength density M satifies $Ma/D = 4.9$. Using the first six modes accounts for nearly 98% of the total relative intensity. The remaining 2% involves modes with very short decay times.

n	β_n	T_n(ms)	I_n(%)
0	1.401	45.00	88.39
1	2.856	10.84	0.80
2	4.332	4.71	6.83
3	5.831	2.60	0.01
4	7.349	1.63	1.75
5	8.874	1.12	0.01
			97.8 Total

It turns out that R must be larger than 2.37 [otherwise it is impossible to satisfy (35b)]. Several values of $R \geq 2.37$ were tried; the best decay curve (as judged by eye) was with $R = 3$ ($R = 3.5$ almost as good). Figure 5 shows this decay curve for $R = 3$; the agreement with the experimental data is very good. The corresponding sink strength parameter is $Ma/D = 4.9$ which, if there were no other surface sinks, would correspond to the intermediate-diffusion region. Table II lists some of the numerical quantities associated with this model. Note, in particular, the alternation in the intensities with n. This is to be expected from such a model with two different nonzero sinks. The small $n = 1$ mode especially helps the agreement with the data since it contributes almost 1% and has a relatively long decay time (10 ms). There is no analog of this mode for the three geometries considered in Sec. II. A total of six modes were used to generate Fig. 5; these account for nearly 98% of the total relative intensity. Presumably the remaining 2% resides in the higher modes whose decay times are very short.

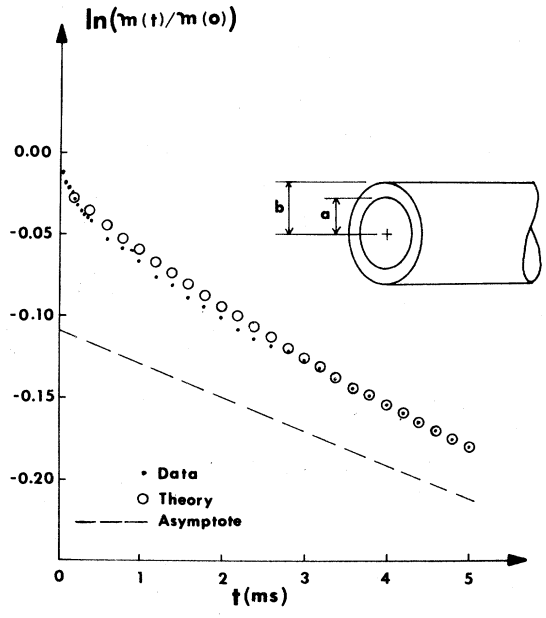

FIG. 5. Decay curve of Hazelwood *et al.* (dots) and its asymptote (dashed line). The open circles are the prediction of the present diffusional theory for the case of an annular cylindrical geometry ($a \leq r \leq b$). The inner surface ($r = a$) is assumed to be infinitely active ($M_{\text{inner}} = \infty$). The figure is drawn for the case $R = b/a = 3.0$; once this free parameter R is chosen the outer surface sink strength is determined by demanding that the theory have the correct asymptote. In this case the outer surface ($r = b$) sink strength is given by $M_{\text{outer}}\, a/D = 4.90$.

Using (36b) one can now solve for the diameter $d=2Ra$ of the cell,

$$d=2R\beta_0(T_0D)^{1/2}. \tag{37}$$

With $D=2.43\times10^{-5}$ cm^2 s^{-1}, $R=3$, $T_0=45$ ms, $\beta_0=1.401$ (from Table II) Eq. (37) gives

$$d=88\ \mu\text{m}, \tag{38}$$

in excellent agreement with the actual diameter of the rat gastronemius cell.[12] [The result (38) is not very sensitive to the choice $R=3$; using $R=3.5$ (a 17% increase) resulted in an increase of d of only about 8%. This is due to a compensating change in β_0].

There could be some disagreement as to the correct value of the diffusivity D which should be used in this type of calculation. We have used $D=2.43\times10^{-5}$ cm^2 s^{-1} which is the bulk value of D for distilled water according to Trappeniers *et al.*[13] and Simpson *et al.*[14] According to Finch *et al.*[12] the value of D is smaller by about a factor of 2 in this type of biological cell and for major fraction decay times of the order of 45 ms. This opinion seems to be shared by Hazelwood *et al.*[1] If we accept this at face value then the cell diameter result, (38), must be reduced by a factor of $\sqrt{2}$ to $d=62$ μm. While we do not disagree that the apparent D for small samples is less than the bulk value by about a factor of 2, it is quite possible that this decrease is simply another manifestation of the very diffusional modes effect discussed in the present article. To quote Wayne and Cotts[15] concerning the reduced value of D: "This does not imply that the real self-diffusion coefficient depends in any way on sample size,... ." Thus it is our point of view that the bulk value of D is the correct one to use.

V. CONCLUSION

The general features of proton-magnetic-resonance data for water in biological cells seem to be adequately described by the simple diffusional model outlined above. In particular, the details of the multiexponential decay characteristic of cells are seen to be a consequence of their size and shape. The only property of water used is the bulk diffusion constant. The relaxation mechanism is modeled by volume and surface like "sinks" whose details are unimportant.

As an example, a "case study" was made of data of Hazelwood *et al.*[1] for rat gastronemius. The assumed geometry was that of an annular cylinder with an infinitely large surface sink strength at the inner surface and a finite surface sink strength at the outer surface. Once the model was fitted to predict the correct large time dependence, it had but one free parameter (ratio of outer to inner radii). The model gave an excellent fit to the data and, together with the known diffusivity of bulk water, furnished the correct cell diameter (88 μm for rat gastronemius).

ACKNOWLEDGMENTS

We wish to thank James A. Rooney and Phillip A. Casabella for several illuminating discussions on this topic.

[1]C. F. Hazelwood, D. C. Chang, B. L. Nichols, and D. E. Woessner, Biophys. J. 14, 583 (1974) and references therein.
[2]C. K. Daszkiewicz, J. W. Hennell, B. Lubas, and T. W. Szczepkowski, Nature (London) 200, 1006 (1963).
[3]R. Cooke and R. Wien, Biophys. J. 11, 1002 (1971).
[4]J. G. Diegel and M. M. Pintar, Biophys. J. 15, 855 (1975).
[5]R. A. Brooks, J. H. Battocletti, A. Sances, Jr., S. J. Larson, R. L. Bowman, and V. Kudravcev, IEEE Trans. Biomed. Eng. 22, 12 (1975).
[6]K. R. Foster, H. A. Resing, and A. N. Garroway, Science 194, 324 (1976).
[7]A. Zipp, I. D. Kuntz, and T. L. James, J. Magn. Reson. 24, 411 (1976).
[8]M. M. Civan, A. M. Achlama, and M. Shporer, Biophys. J. 21, 127 (1978).
[9]K. R. Brownstein, J. Maine Med. Assn. 68, 252 (1977).
[10]J. R. Zimmerman and W. E. Brittin, J. Phys. Chem. 61, 1328 (1957).
[11]K. R. Brownstein and C. E. Tarr, J. Magn. Reson. 26, 17 (1977).
[12]E. D. Finch, J. F. Harmon, and B. H. Muller, Arch. Biochem. Biophys. 147, 299 (1971).
[13]N. J. Trappeniers, C. J. Gerritsma, and P. H. Oosting, Phys. Lett. 18, 256 (1965).
[14]J. H. Simpson and H. Y. Carr, Phys. Rev. 111, 1201 (1958).
[15]R. C. Wayne and R. M. Cotts, Phys. Rev. 151, 264 (1966).